Acta Cryst. (1982). A**38**, 841–848

Theoretical Considerations on Phase Determination by Three-Beam Interference

BY K. HÜMMER AND H. W. BILLY

Institut für Angewandte Physik, Lehrstuhl Kristallographie, Universität Erlangen–Nürnberg, Loewenichstrasse 22, D 8520 Erlangen, Federal Republic of Germany

(*Received* 26 *April* 1982; *accepted* 23 *June* 1982)

Abstract

For φ-scan experiments rotating the crystal through a three-beam case the rocking-curve profiles have been calculated on the basis of the dynamical theory of X-ray diffraction. Divergence and wavelength spread of the incident beam have been taken into account. It is shown that for centrosymmetric crystal structures the asymmetry of the profiles is related to the sign of the triple product of the structure factors $F(\bar{\mathbf{h}})F(\mathbf{g})F(\mathbf{h}-\mathbf{g})$ which are involved in a three-beam case. If anomalous absorption ('double Borrmann' effect) can be neglected the typical asymmetry is independent of the diffraction geometry (Laue or Bragg case). For Laue geometry and thick crystals ($\mu_0 t > 1$) corrections are necessary. For centrosymmetric structures it may be possible to determine the phase sum of a triplet by inspection of the rocking curve without computer calculations. The general features of the rocking curve are discussed and a physical interpretation is given.

1. Introduction

It has been suggested for a long time that, in X-ray and electron multiple diffraction processes where several Bragg reflections are excited simultaneously, the intensities of the diffracted beams depend on the relative phases of the structure factors involved (Lipscomb, 1949; Kambe, 1957; Hart & Lang, 1961; Colella, 1974; Post, 1979; Chapmann, Yoder & Colella, 1981; Chang, 1982). Particularly for the three-beam case where two reciprocal-lattice points (r.l.p.'s) H and G lie simultaneouly close to or on the Ewald sphere besides the origin O of the reciprocal space, attempts have been made to deduce information on the phases from the observed reflection anomalies (*Aufhellung* and *Umweganregung*). The intensities of the three-beam reflections are, in fact, influenced by the interference effects of the scattered waves. For instance, the directly excited wave diffracted at the lattice plane (**h**) and the detour excited wave successively reflected at the lattice planes (**g**) and (**h** − **g**) are propagated in the same direction. The amplitude of the resulting wave depends on the difference of the phases of both waves:

$$\Phi_\Sigma = \pm[-\varphi(\mathbf{h}) + \varphi(\mathbf{g}) + \varphi(\mathbf{h}-\mathbf{g})]. \qquad (1)$$

This kinematical approach cannot adequately describe the amplitudes of the self-consistent wave field established by all possible combinations of coupling of the three beams. There are also couplings which are independent of the phase sum Φ_Σ. Moreover, anomalous absorption effects (Borrmann effect) may suppress the phase effect. Therefore the phenomenon of multiple diffraction must be treated on the basis of dynamical theory. As was pointed out by Ewald & Héno (1968) in the dynamical theory for the three-beam case too, the phase-dependent terms only contain the sum of phases Φ_Σ, *i.e.* the physical results are independent of the choice of the origin for describing the crystal structure.

Information on the phase sum Φ_Σ may be provided by the profile of a ψ-scan rocking curve at the transition from the two-beam to the three-beam case (Billy & Hümmer, 1981). A suitable technique to measure this effect is the so called ψ-scan experiment in which the crystal is rotated around the direction of a vector **h** of the reciprocal lattice. The corresponding r.l.p. H lies on or very close to the Ewald sphere, and on rotating the crystal a second r.l.p. G crosses the sphere. While G moves through, the diffracted intensity of the **h** reflection is measured.

In centrosymmetric crystal structures the phase sum Φ_Σ of a triplet of structure factors can only be zero or π, corresponding to a positive or negative sign of the triple product $F(\bar{\mathbf{h}})F(\mathbf{g})F(\mathbf{h}-\mathbf{g})$ (in short: positive or negative triplet), if one neglects the imaginary part of the atomic scattering factor. The question arises whether the rocking-curve line shape is connected with this sign.

To study this relation we calculated three-beam rocking curves based on von Laue's formulation of the dynamical theory. As a model crystal structure we chose α-Al_2O_3 (space group $R\bar{3}c$) in which positive and negative triplets with comparable structure amplitudes exist.

0567-7394/82/060841-08$01.00

In a first approximation an ideal monochromatic and parallel incident beam is assumed. In a second step these restrictions are removed in order to evalute the experimental verification under more realistic conditions. In the third section we discuss the results on a simplified mathematical basis and give a physical interpretation of the general features of the three-beam rocking curve.

2. Calculation of the rocking-curve profile

(a) *Theory and computational details*

The interaction between X-rays and a perfect crystal will be described within the scheme of the dynamical theory by Maxwell's equations for a medium with a periodic complex dielectric constant combined with the boundary conditions at the entrance and exit surfaces. The solution of Maxwell's equations are given by the solutions of the fundamental equations of the dynamical theory which describe the self-consistently coupled wave fields inside the crystal (Laue, 1960):

$$\frac{K_n^2 - k^2}{K_n^2}\,\mathbf{D}_n = -\Gamma \sum_m F(\mathbf{n}-\mathbf{m})\,\mathbf{D}_{m[n]}. \qquad (2)$$

Concerning the three-beam case, (2) leads to a set of three vector equations with $\mathbf{m}, \mathbf{n} = \mathbf{0}, \mathbf{h}, \mathbf{g}$. $\mathbf{0}$ is a vector of zero length; $\mathbf{h}$, $\mathbf{g}$ are the vectors of the reciprocal lattice to the r.l.p.'s H, G; k is the length of the vacuum wave vector. $\mathbf{K}_n$ is the complex wave vector inside the crystal, directed towards a reciprocal-lattice point; $\mathbf{D}_n$ is the amplitude of the dielectric displacement vector of the wave with $\mathbf{K}_n$; $\mathbf{D}_{m[n]}$ is the component of $\mathbf{D}_m$ perpendicular to $\mathbf{K}_n$; $F(\mathbf{n}-\mathbf{m})$ are the structure factors with *complex* atomic scattering factors. Γ is a number of the order of 10^{-5}.

The unknowns in these equations are $\mathbf{K}_n$ and $\mathbf{D}_n$. For the numerical calculation of the surface of dispersion (surface of dispersion is the loci of the end-points of all permitted $\mathbf{K}_n$) and of the relative excitation amplitudes $\mathbf{D}_n$, it is convenient to transcribe (2) in an eigenvalue problem. This procedure is already described in the literature (Pinsker, 1978, pp. 422–430), but for the self-consistency of this paper the essential steps will be outlined. This may be helpful for the understanding of the further discussion.

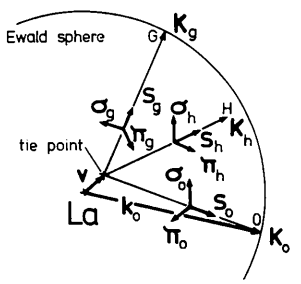

Fig. 1. The position of the Laue point La and one tiepoint, wave vectors $\mathbf{K}_n$ and polarization vectors $\boldsymbol{\sigma}_n$, $\boldsymbol{\pi}_n$ in reciprocal space.

In order to describe the position of the surface of dispersion in reciprocal space a complex vector $\mathbf{v}$ is introduced, which leads from the three-beam Laue point La (center of the Ewald sphere with radius k) to the end-point of $\mathbf{K}_n$ (tiepoint) on the surface of dispersion (*cf.* Fig. 1). The position of the Laue point itself is given by $\mathbf{k}_0$ from La to the origin O. Thus, $\mathbf{k}_0$ gives the direction of the incident beam for the exact three-beam setting and the following relations hold:

$$\begin{aligned} &\mathbf{K}_0 = \mathbf{k}_0 - \mathbf{v}, \quad \mathbf{K}_n = \mathbf{K}_0 + \mathbf{n}, \\ &\mathbf{k}_n = \mathbf{k}_0 + \mathbf{n}, \quad \mathbf{n} = \mathbf{h}, \mathbf{g}. \end{aligned} \qquad (3)$$

$\mathbf{k}_0$ can be calculated according to the formula given by Ewald & Héno (1968).

Because of the continuity of the tangential components of the wave vectors, $\mathbf{k}_0$ and $\mathbf{K}_0$ can only differ in the component perpendicular to the crystal surface. They are related by

$$\mathbf{K}_0 = \mathbf{k}_0 - (\mathbf{x}.\mathbf{v})\,\mathbf{x}. \qquad (4)$$

$\mathbf{x}$ is a unit vector in reciprocal space normal to the crystal surface and directed inwards from the surface. By two additional unit vectors $\mathbf{y}$, $\mathbf{z}$ lying in a plane parallel to the crystal surface a Cartesian base is set up, the origin of which is the Laue point.

As the vacuum wave vector $\mathbf{k}_0$ is not complex, only the component v_x of $\mathbf{v}$ can be complex and its imaginary part v_x'' is proportional to the absorption coefficient. From (3) and (4), (2) can be written as:

$$\begin{aligned} &[a(\mathbf{k}_n.\mathbf{v}) - \Gamma F(\mathbf{0})]\mathbf{D}_n = \Gamma \sum_{m \neq n} F(\mathbf{n}-\mathbf{m})\mathbf{D}_{m[n]}; \\ &\mathbf{m}, \mathbf{n} = \mathbf{0}, \mathbf{h}, \mathbf{g}, a = 2[1 + \Gamma F(\mathbf{0})]k_0^{-2} \end{aligned} \qquad (5)$$

Second-order terms of v can be neglected. They are of the order of 10^{-6} compared with k_n^2 for small deviations from the three-beam setting ($\leq 5'$). With this approximation only those beams are considered which are selected by the Ewald construction, *i.e.* specular reflected waves are omitted assuming larger glancing angles than the critical angle for total reflexion (Kishino & Kohra, 1971). Then equations (2) reduce to a linear system of equations (5).

As can be seen in the funamental equations (2), the coupling between two waves $\mathbf{D}_m$ and $\mathbf{D}_n$ depend on the structure factor $F(\mathbf{n}-\mathbf{m})$ and on the diffraction geometry by the component $\mathbf{D}_{m[n]}$, which is given by

$$\mathbf{D}_{m[n]} = \mathbf{D}_m - \mathbf{s}_n.(\mathbf{D}_m.\mathbf{s}_n); \quad \mathbf{s}_n = \mathbf{K}_n/|\mathbf{K}_n|. \qquad (6)$$

Since $\mathbf{D}_n$ is always perpendicular to $\mathbf{s}_n$ only two components can be chosen independently:

$$\mathbf{D}_n = D_n^{\sigma}\,\boldsymbol{\sigma}_n + D_n^{\pi}\,\boldsymbol{\pi}_n. \qquad (7)$$

$\mathbf{s}_n$, $\boldsymbol{\pi}_n$, $\boldsymbol{\sigma}_n$ form a Cartesian base. The unit vectors $\boldsymbol{\sigma}_n$ and $\boldsymbol{\pi}_n$ can be arbitrarily aligned, but it is convenient to regard all vectors $\boldsymbol{\pi}_n$ lying in the plane of $\mathbf{K}_0$ and $\mathbf{K}_h$ as shown in Fig. 1.

The geometrical coupling between the components of $\mathbf{D}_n$ can now be expressed in terms of scalar products of $\boldsymbol{\pi}_n$ and $\boldsymbol{\sigma}_n$. If (6) and (7) are inserted in (5) and then multiplied by $\boldsymbol{\sigma}_n$ and $\boldsymbol{\pi}_n$ respectively for the components D_n^σ and D_n^π a set of linear scalar equations results:

$$b_n D_n^\sigma + \frac{1}{ak_n^x} \Gamma \sum_{m \neq n} F(\mathbf{n}-\mathbf{m})\,(D_m^\sigma\, \boldsymbol{\sigma}_m\, \boldsymbol{\sigma}_n + D_m^\pi\, \boldsymbol{\pi}_m\, \boldsymbol{\sigma}_n) = v_x D_n^\sigma$$

$$b_n D_n^\pi + \frac{1}{ak_n^x} \Gamma \sum_{m \neq n} F(\mathbf{n}-\mathbf{m})\,(D_m^\sigma\, \boldsymbol{\sigma}_m\, \boldsymbol{\pi}_n + D_m^\pi\, \boldsymbol{\pi}_m\, \boldsymbol{\pi}_n) = v_x D_n^\pi \qquad (8)$$

with

$$b_n = -\frac{k_n^y v_y + k_n^z v_z}{k_n^x} + \frac{\Gamma F(\mathbf{0})}{ak_n^x};\ \mathbf{m}, \mathbf{n} = \mathbf{0}, \mathbf{h}, \mathbf{g}.$$

This eigenvalue problem can be written in the form

$$SY(j) = v_x(j)\, Y(j). \qquad (9)$$

For the three-beam case S is a six by six matrix and for each eigensolution $v_x(j)$ (j = 1 to 6) the components of $Y(j)$ are given by $Y(j) = [D_0^\sigma(j), D_0^\pi(j), D_h^\sigma(j), D_h^\pi(j), D_g^\sigma(j), D_g^\pi(j)]$.

Only one component of $\mathbf{v}$ can be determined by (8), which according to (4) must be v_x. The tangential components v_y and v_z depend only on the direction of the incident beam. In order to relate the input parameters to the crystal orientation in a ψ-scan experiment, a new two-dimensional coordinate system is introduced with the mutually orthogonal unit vectors $\mathbf{a}_1$ and $\mathbf{a}_2$ with its origin at the Laue point. The vectors $\mathbf{a}_1$ and $\mathbf{a}_2$ lie on a plane normal to $\mathbf{k}_0$, that is the tangential plane at La on a sphere of radius $|\mathbf{k}_0|$ around O (see Fig. 2). The component ψ in the direction of $\mathbf{a}_1$ should describe the rotation angle ψ of the crystal around the direction of $\mathbf{h}$. Therefore, $\mathbf{a}_1$ lies in the plane perpendicular to $\mathbf{h}$ and passing through the midpoint of $\mathbf{h}$. The component Ω of $\mathbf{a}_2$ defines the deviation of $\mathbf{h}$ from the Ewald sphere. $\psi = \Omega = 0$ gives the exact three-beam setting. Then $\mathbf{v}$ is given by

$$\mathbf{v} = v_x\, \mathbf{x} + \hat{\mathbf{v}};\quad \hat{\mathbf{v}} = \psi \mathbf{a}_1 + \Omega \mathbf{a}_2. \qquad (10)$$

The projection of $\hat{\mathbf{v}}$ along $\mathbf{x}$ onto the (y,z) plane gives the components v_y and v_z.

The solutions of the eigenvalue problem were obtained by numerical methods using subroutines of the software package *EISPACK* of CERN modified for a PDP 11/45.

If the calculated relative components of the eigenvectors $Y(j)$ are inserted into the boundary conditions, the absolute values of $D_n^{\sigma,\pi}(j)$ can be determined. The boundary conditions for a parallel-sided crystal slab are summarized in Table 1. They depend on whether at the entrance surface the wave vectors $\mathbf{K}_n$ ($n = h, g$) of the diffracted beams are directed into the crystal ($\mathbf{K}_n.\mathbf{x} > 0$, Laue case) or out from the crystal ($\mathbf{K}_n.\mathbf{x} < 0$, Bragg case). It is assumed that no refraction takes place at the boundaries. The amplitude of the incident beam is taken as unity.

If there are N_{Br} Bragg cases involved in an N-beam case, there will exist tiepoints, the waves of which have a negative absorption coefficient [$\mu(j) < 0$]. This is equivalent to the fact that the Poynting vectors $\mathbf{S}(j)$ of these modes are directed outwards from the entrance surface. These modes are called 'forbidden modes'. The number N_p of permitted propagation modes is given by (Pinsker, 1978, p. 478)

$$N_p = 2(N - N_{Br}). \qquad (11)$$

For thick crystals the forbidden modes have no physical meaning because their wave amplitudes increase exponentially with the distance from the entrance surface. They will be eliminated by the boundary conditions at the exit surface (Table 1).

With the known amplitudes $D_n^{\sigma,\pi}(j)$ the energy flow in the direction of $\mathbf{k}_n$ outside the crystal can be calculated by summing up the intensities of the individual waves:

$$I_n(\psi, \Omega) = \tfrac{1}{2} \sum_j [D_n^\sigma(j)^2 + D_n^\pi(j)^2] \exp[-2\mu(j)\, t]. \qquad (12)$$

Equation (12) is valid when the following conditions hold. The incident beam is unpolarized. Neither *Pendellösung* interference phenomena nor the spatial distribution of intensities within the fan of beams at the exit surface need to be considered. The latter conditions will be discussed in more detail in § 2(*c*). For very thin crystals (t less than a *Pendellösung* period) and a strictly parallel and monochromatic incident beam (12) is not valid. Hence amplitudes rather than intensities must be summed:

$$I_n(\psi, \Omega) = \tfrac{1}{2} \left| \sum_j D_n^\sigma(j) \exp[2\pi i\, \mathbf{K}_n(j).\mathbf{r}] \right|^2 + \tfrac{1}{2} \left| \sum_j D_n^\pi(j) \exp[2\pi i\, \mathbf{K}_n(j).\mathbf{r}] \right|^2 \qquad (13)$$

$$\mathbf{K}_n(j) = k_0 + n - v(j).$$

Table 1 *Boundary conditions*

$\mu(j) = 4\pi v_x''(j)$: absorption coefficient of the waves for the jth tiepoint.
t: thickness of the parallel-sided crystal slab.

	Entrance surface	Exit surface
$n = 0$	$\sum_j D_0(j) = 1$	–
$n = h, g$ Laue case	$\sum_j D_n(j) = 0$	–
Bragg case	–	$0 = \sum_j D_n(j) \exp[-\tfrac{1}{2}\mu(j)t]$

(b) Results

By use of the procedure described above we calculated the ψ-scan rocking curves $I_h(\psi,\Omega)$ = constant) of several three-beam cases for the centrosymmetric structure α-Al_3O_3 (space group $R\bar{3}c$). To a first approximation the calculations are based on the assumption of an ideal monochromatic (Cu $K\alpha$: λ = 1·54 Å) and completely parallel collimated incident beam. In § 2(*c*) these restrictions are removed. Examples of typical results for a positive and negative triplet are shown in Figs. 2 and 3, where for comparison in each case rocking-curve profiles of the **h** = 110 reflection are drawn for different diffraction geometries. The theoretical values I_{110} have been normalized with respect to its two-beam intensity $I^{(2)}_{110}$. The notation Laue–Bragg, for instance, means that the diffracted beams with wave vectors $\mathbf{K}_h$ and $\mathbf{K}_g$ represent Laue and Bragg cases respectively.

The structure factors of the selected triplets should have equal values and medium strength compared to $F(\mathbf{0})$. Therefore, we chose the positive triplet with $\bar{\mathbf{h}}$ = $\bar{1}\bar{1}0$, $\mathbf{g} = 2\bar{1}0$, $\mathbf{h} - \mathbf{g} = \bar{1}20$ and the negative triplet with $\bar{\mathbf{h}} = \bar{1}\bar{1}0$, $\mathbf{g} = 2\bar{1}\bar{3}$, $\mathbf{h} - \mathbf{g} = \bar{1}23$. The components *hkl* refer to the hexagonal setting. The values of the structure factors are:

$$F(000) = 303, \quad F(\bar{1}\bar{1}0) = F(2\bar{1}0) = F(\bar{1}20) = 63,$$
$$F(2\bar{1}\bar{3}) = F(\bar{1}23) = 76.$$

The positive $\mathbf{a}_1$ direction is always defined such that the r.l.p. G enters the Ewald sphere, *i.e.* G moves from outside ($\psi < 0$) to inside ($\psi > 0$) the sphere (Chang, 1982) (out–in case).

Figs. 2(*a*) and (*b*) indicate that the asymmetry of the line profiles is definitely related to the sign of the triplet. If the crystal is rotated in the out–in direction for the case of a positive triplet, the intensity is first increased, when G approaches the Ewald sphere, and is lowered, when G moves away from it. Just the opposite holds for a negative triplet. The parameter $\Omega \neq 0$ indicates that **h** is slightly off the exact two-beam setting so that the two-beam intensity is about 50% of its maximum value. Concerning the rocking curves for the Laue–Bragg and Bragg–Laue geometry, which are not drawn here, we have obtained equivalent results. Hence the general features of the rocking curves do not depend on the direction of the surface normal of the crystal. For our calculations we chose symmetrical Laue and nearly symmetrical Bragg geometry with respect to the **h** reflection.

The influence of the anomalous absorption (enhanced Borrmann effect) is different for the Laue and Bragg diffraction geometries. As for the Bragg–X cases, the intensity is hardly affected by absorption effects because the Bragg-reflected beam does not enter the crystal. However, in Laue–X cases the anomalous absorption may drastically change the rocking-curve profile. This is illustrated in Fig. 3 where for a Laue–Laue case rocking curves are shown with different parameters $\mu_0 t$. (μ_0 is the absorption coefficient in the one-beam case; for Al_2O_3, μ_0 = 121

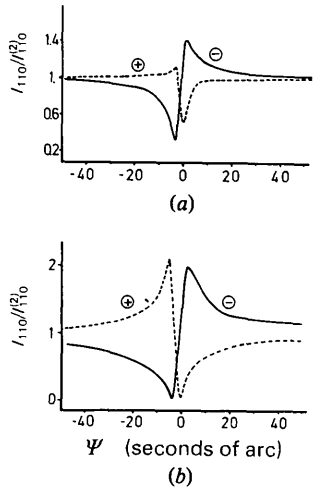

Fig. 2. (*a*) Rocking-curve profiles $I(\psi, \Omega = 2{\cdot}5'')$ for a Laue–Laue case for a positive (dashed line, ⊕) and a negative triplet (full line, ⊖); $\mu_0 t = 1{\cdot}3$. (*b*) rocking-curve profiles $I(\psi, \Omega = 10'')$ for a Bragg–Bragg case for a positive (dashed line) and a negative triplet (full line); $\mu_0 t = 3{\cdot}9$.

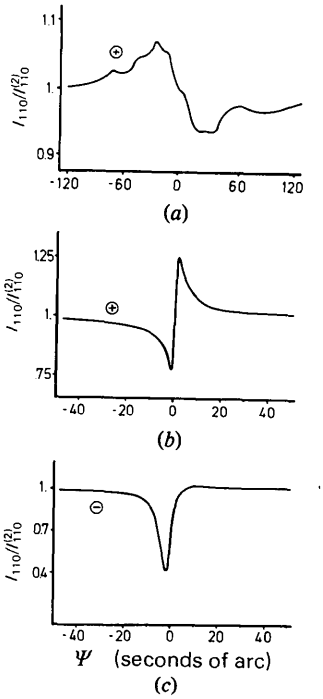

Fig. 3. Rocking-curve profiles $I(\psi, \Omega = 0)$ for a Laue–Laue case for equal triplets as in Fig. 2: (*a*) positive triplet, $\mu_0 t = 0{\cdot}01$; (*b*) positive triplet, $\mu_0 t = 1{\cdot}3$; (*c*) negative triplet, $\mu_0 t = 1{\cdot}3$.

cm^{-1}.) In contrast to Fig. 2, $\Omega = 0$, *i.e.* the two-beam setting is on its maximum value.

In Fig. 3(*a*), for an unreasonably thin crystal with $t = 1$ μm [calculation according (13)], the influence of anomalous absorption is negligibly small. The asymmetry is that typical for a positive triplet, the small oscillations are due to interference effects of the diffracted waves. The characteristic asymmetry is hardly affected by this *Pendellösung* phenomenon. By use of (12) the same type of asymmetry is obtained.

For a thicker crystal with $t = 0{\cdot}1$ mm the enhanced Borrmann effect completely changes the typical profile (Fig. 3*b*). For comparison, in Fig. 3(*c*) the rocking curve is drawn for a negative triplet. As can be seen by comparing Figs. 3(*b*) and 2(*a*) with equal parameter $\mu_0 t$, the anomalous absorption effect is much weaker when the wave field with $\mathbf{K}_h$ is not fully excited ($\Omega \neq 0$). The influence of the Borrmann effect on the profile depends on the deviation of the absorption coefficient from its two-beam value which is largest near the exact three-beam setting ($\Omega = 0$, $\psi = 0$), and on the excitation amplitudes of the waves.

When the two-beam intensity level is at its maximum value, then essentially a dip (*Aufhellung*) can be observed in the three-beam rocking curve (Fig. 3*c*). (Note that for the Bragg case the maximum two-beam intensity is shifted from the exact two-beam setting $\Omega = 0$.)

In conclusion, the results can be summarized as follows:

(i) When the influence of the anomalous absorption is negligibly small the asymmetry of the three-beam rocking-curve profile is strictly related to the sign of the triplet independent of the diffraction geometry. Therefore it is:

$$I_n^+(-\psi)/I_n^{(2)\prime} > I_m^-(-\psi)/I_m^{(2)}$$

and

$$I_n^+(\psi)/I_n^{(2)} < I_m^-(\psi)/I_m^{(2)}.$$

If it is known whether the r.l.p. G moves towards or away from the Ewald sphere (Chang, 1982) while the crystal is rotated, the sign of the triplet can be determined by a ψ-scan experiment without computer calculations.

(ii) In the case that the anomalous absorption effects cannot be neglected, there is also a clear difference between the rocking-curve line shape of a positive and a negative triplet (*cf.* Figs. 3*b* and *c*). Comparison with the calculated profile may be necessary in order to extract the phase information.

(iii) The influence of the anomalous absorption can be reduced when the two-beam setting of the diffraction vector $\mathbf{h}$ is slightly off the Ewald sphere. Then additionally the asymmetry is more pronounced because the increase of the two-beam level is larger.

(c) Effect of divergence and spectral width of the incident beam

The calculations so far have been based on the following assumptions: (i) neglect of *Pendellösung* interference phenomena as well as neglect of the different directions of energy flow given by the Poynting vectors $\mathbf{S}(j)$ of each mode; (ii) no divergence of the incident beam; (iii) ideal monochromatic X-ray source.

For comparison of the theoretical results with measurements under realistic conditions, point (i) is no restriction. In practice, the irregularities in the thickness of the crystal produce an averaging effect over the *Pendellösung* periods. Moreover, the incident beam is divergent and a wide fan of diffracted beams is formed in the crystal. If the entrance slit of the detector is larger than the diameter of the diffracted beam the detector will integrate over the spatial distribution of the diffracted rays within the fan. In both cases, the waves can be treated separately and intensities (proportional to $D_n^{\sigma,\pi 2}$) rather than amplitudes add for the exit beam (Batterman & Cole, 1964). Then, to measure the rocking curve the crystal has to be rotated since the angular resolution of the detector is only poor. The detector remains in a fixed position.

The divergence and spectral width having been taken into account, the total power $I(\psi)$ reflected by the crystal must be calculated by integrating over the angular range α of divergence and over the wavelength spread $\Delta\lambda$. The angular distribution of the intensity is represented by the geometrical function $G(\alpha)$, which in general varies only slowly with α and can be considered to be a constant. The wavelength spread is given by the spectral function $S(\lambda - \lambda_0)$; λ_0 is the wavelength corresponding to the center of the characteristic line.

The variation of the wavelength yields a variation $\Delta\mathbf{k}_0$ of the three-beam Laue point La. Decomposition of $\Delta\mathbf{k}_0(\lambda)$ in the direction of $\mathbf{a}_1$, $\mathbf{a}_2$ and $\mathbf{s}_0$ gives the angular difference $\Delta\psi(\lambda)$ and $\Delta\Omega(\lambda)$ between the exact three-beam settings with respect to the wavelengths λ_0 and λ.

With the angular terms due to divergence ($\alpha_\psi, \alpha_\Omega$) and an additional crystal rotation ψ the integrated intensity $I(\psi)$ is given by (Alexander & Smith, 1962):

$$I(\psi) = G(\alpha_\Omega)\, G(\alpha_\psi) \int_{\alpha_1}^{\alpha_2} \mathrm{d}\alpha_\Omega \int_{\alpha_1}^{\alpha_2} \mathrm{d}\alpha_\psi \int_{\lambda_1}^{\lambda_2} \mathrm{d}\lambda' S(\lambda_0 - \lambda')$$

$$\times \int_{\lambda_1}^{\lambda_2} \mathrm{d}\lambda'' S(\lambda_0 - \lambda'')\, I[\alpha_\psi - \Delta\psi(\lambda'')$$

$$+ \psi, \alpha_\Omega - \Delta\Omega(\lambda')]. \qquad (14)$$

The reduction of these convolution integrals is similar to that given by James (1948) for a double-crystal

spectrometer:

$$I(\psi) = \text{constant} \times \int_{-\infty}^{+\infty} d\alpha_\Omega \int_{\alpha_1}^{\alpha_2} d\alpha_\psi \int_{\lambda_1}^{\lambda_2} d\lambda'' S(\lambda_0 - \lambda'') \times I[\psi + \alpha_\psi - \Delta\psi(\lambda''), \alpha_\Omega]. \quad (15)$$

This derivation is valid when no monochromator crystal is used. It should be noted that the angular range $\Delta\psi(\lambda)$ due to the spectral width can be reduced when $\Delta\mathbf{k}_0(\lambda)$ has only a small component in the direction of $\mathbf{a}_1$, *i.e.* $\mathbf{k}_0(\lambda)$ is nearly parallel to $\mathbf{k}_0(\lambda_0)$. This can be achieved with small diffraction vectors **h** and **g**.

By use of (15) we calculated the integrated reflected power $I(\psi)$ for the same diffraction geometries and the same triplets as in § 2(*b*). The angular range of divergence of the incident beam was assumed to be $\alpha = 2'$. The spectral function $S(\lambda - \lambda_0)$ was considered to be Gaussian-like and the half-width of the Cu $K\alpha$ line of $\Delta\lambda/\lambda = 3 \times 10^{-4}$ (Pinsker, 1978, p. 284) gives an angular range $\Delta\psi = 18''$ and $\Delta\psi = 13''$ for the positive and negative triplet respectively. The numerical integration over Ω is carried out in an interval for which the ratio $I(\psi_1,\Omega_1)/I_{\max}(\psi_1,\Omega_0) \gtrsim 10^{-3}$.

Evaluation of the integral (15) for the Bragg–Bragg case is expected to give no significant change of the asymmetry because the integral with respect to Ω is taken over profiles with nearly the same sense, *i.e.* for a negative triplet, for instance, for each Ω the rocking curve $I(\psi, \Omega = \text{constant})$ first decreases and then increases. By integration the variation of the two-beam intensity is reduced to the order of some few percent and the width of the profile is increased. The results are illustrated in Fig. 4(*a*). Inspection of Figs. 2(*a*) and 3(*c*) reveals that the same arguments hold for the Laue–Laue geometry and a negative triplet, as shown in Fig. 4(*b*).

But in the case of a positive triplet the behavior of the rocking curve is different when $\mu_0 t \gtrsim 1$. The integral over Ω runs over line shapes with different asymmetries (compare Figs. 2*a* and 3*b*). As a consequence, by integration the characteristic rocking-curve profile may vanish. The result is illustrated in Fig. 4(*b*) and shows only a small decrease of the two-beam intensity, of the order of 1%. The different behavior for positive and negative triplets in the case of a thick crystal has already been discussed by Post (1979). Careful inspection of the excitation amplitudes shows that this difference must be due to absorption. For a positive triplet there are four sheets of the surface of dispersion with a lowered absorption coefficient and only two sheets for a negative triplet. The characteristic profile of the latter is therefore less affected by the thickness of the crystal.

If the influence of anomalous absorption can be neglected the profile shows the characteristic asymmetry for a positive triplet too. This may be important in the case of a mosaic crystal where dynamical theory is valid within each mosaic grain and the size of these blocks will reduce the anomalous absorption effects.

The profiles of Figs. 4(*a*) and (*b*) are typical ones for three nearly equal structure factors. If the structure factor $F(\mathbf{h})$ is small compared with $F(\mathbf{g})$ and $F(\mathbf{h} - \mathbf{g})$ only an increase of the low two-beam intensity level can be observed (*Umweganregung*) and it is difficult to determine unambiguously the sense of the asymmetry. If, on the other hand, $F(\mathbf{h})$ is large only a dip will appear and the same difficulties arise.

It should be noted that the profile is completely smeared out if the divergence of the incident beam is too large.

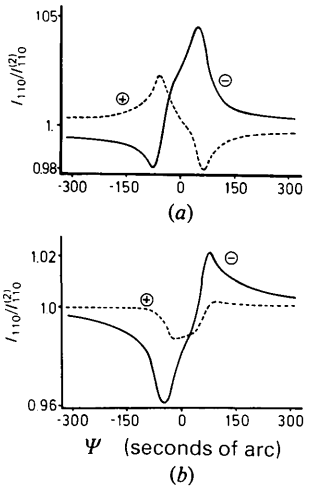

Fig. 4 (*a*) Integrated rocking-curve profiles $I(\psi)$ for the same Bragg–Bragg case as in Fig. 2(*b*); $\mu_0 t = 3{\cdot}9$. (*b*) Integrated rocking-curve profiles $I(\psi)$ for the same Laue–Laue case as in Fig. 2(*a*), $\mu_0 t = 1{\cdot}3$.

3. Discussion

In this section we discuss the general features of the ψ-scan rocking curve for the three-beam case on a simplified mathematical basis. A physical interpretation is given.

The outcome of (8) and (9) reveals that there always exist three pairs of nearly doubly degenerate eigensolutions (Hildebrandt, 1967). The two eigensolutions of each pair essentially correspond to σ and π polarization respectively. Neglecting the geometrical coupling factors $\boldsymbol{\sigma}_n . \boldsymbol{\pi}_m$ the determinant of (8) and (9) can be reduced to three by three for one polarization only. This reduced system of equations now gives the general features of the three-beam case too.

If a hypothetical centrosymmetric structure is assumed where positive and negative triplets exist with equal modulus of structure factors and equal geometrical coupling factors, in the case of a positive (S^+) or a

negative triplet (S^-), the determinant of the reduced system of equations is given by:

$$S^{\pm} = \begin{vmatrix} \tilde{b}_0 - \tilde{v}_x & \alpha_h^0 F(-\mathbf{h}) & \pm\alpha_g^0 F(-\mathbf{g}) \\ \alpha_h^0 F(\mathbf{h}) & \tilde{b}_h - \tilde{v}_x & \alpha_g^h F(\mathbf{h}-\mathbf{g}) \\ \pm\alpha_g^0 F(\mathbf{g}) & \alpha_g^h F(\mathbf{g}-\mathbf{h}) & \tilde{b}_g - \tilde{v}_x \end{vmatrix} = 0, \quad (16)$$

$\tilde{b}_n$ = constant $\times$ $(\tilde{\mathbf{v}}.\mathbf{s}_n)_{y,z}$, $n = 0, h, g$. The negative triplet is obtained by changing the sign of one structure factor (origin at the center of symmetry), for example the sign of $F(\mathbf{g})$ and $F(-\mathbf{g})$. For this discussion the origin of the x,y,z coordinate system is shifted from the Laue point to the Lorentz point (*Lo*), therefore $\tilde{\mathbf{v}}$ is a vector analogous to $\mathbf{v}$ but starting from *Lo*. α_m^n represents the geometric coupling of $\mathbf{D}_m$ and $\mathbf{D}_n$.

If in S^- the direction of $\tilde{\mathbf{v}}$ is inverted ($\tilde{\mathbf{v}} \rightarrow -\tilde{\mathbf{v}}$), that means the signs of the main diagonal elements are changed, the expansion of the determinant S^+ and S^- leads to identical characteristic polynomials for the eigenvalue v_x. Thus, in the special case for a positive and a negative triplet the corresponding surfaces of dispersion are related to each other by inversion at *Lo*.

As the wave fields are determined by the tiepoint on the surface of dispersion which depends on ψ and Ω it must be $I_n^+(\psi,\Omega) = I_n^-(-\psi,-\Omega)$. Therefore, the line profile for a positive triplet $I_n^+(\psi,\Omega_0)$ and the profile for a negative triplet $I_n^-(\psi,-\Omega_0)$ are simply reversed rotating the crystal in the same (*e.g.* out–in) direction.

In a realistic centrosymmetric structure for positive and negative triplets different r.l.p's are involved, *i.e.* different geometrical coupling factors and different structure amplitudes. Thus the inversion of the rocking curve stated above is not exact, but in principle the statement remains true.

Ewald & Héno (1968) have pointed out that for $\Phi_\Sigma = \pm\pi/2$ the dispersion surface is centrosymmetric about the Lorentz point. In such a case the rocking curve must be symmetric. This may be a hint on how to get information on the phase sum in noncentrosymmetric structures.

In the following a physical interpretation is given for the asymmetry of the line profiles. The interference of the coupled waves is considered from a more kinematical point of view in accordance with the original idea of Lipscomb (1949). When two net planes (**h**) and (**g**) are simultaneously in reflection position, there exists not only the direct diffracted wave in the direction of $\mathbf{K}_h$ [amplitude $\gamma_h D_0$, phase $\varphi(\mathbf{h})$], but also a wave which is excited by the successive reflection at the lattice planes (**g**) and (**h** − **g**) [amplitude $\gamma_g D_0$, phase $\varphi(\mathbf{g}) + \varphi(\mathbf{h}-\mathbf{g})$]. Detour reflection of higher order should be neglected here. The superposition of these two waves can approximately be expressed by

$$D_h = \gamma_h(\Omega) D_0 \exp[i\varphi(\mathbf{h})] + \gamma_g(\psi) D_0 \exp i[\varphi(\mathbf{g}) + \varphi(\mathbf{h}-\mathbf{g})]. \quad (17)$$

The factors γ depend on the deviation Ω, ψ from the exact reflection position.

Concerning the excitation amplitudes we refer to the results of the dynamical theory. In a ψ-scan experiment $\gamma_h(\Omega)$ is constant and of the order of one for a nearly symmetric reflection. Varying ψ, $\gamma_g(\psi)$ drops rapidly down to zero from its maximum value which close to $\psi = 0$ is of the order of one too.

Now the phase relationships are considered. In the centrosymmetric cases the interference should be either constructive or destructive depending on Φ_Σ. But the outcome of dynamical theory reveals an additional phase shift of π when the r.l.p. G moves through the Ewald sphere. For a three-beam case this continuous phase shift can be seen in Fig. 5, where for simplicity the phase relationship is shown for one polarization state only. The phase sum $\hat{\Phi}_\Sigma = \hat{\varphi}(\mathbf{h}) - \hat{\varphi}(\mathbf{g}) - \varphi(\mathbf{h}-\mathbf{g})$ is plotted which is given by the calculated actual phases $\hat{\varphi}(\mathbf{h})$ and $\hat{\varphi}(\mathbf{g})$ of the observable waves with wave vectors $\mathbf{K}_h$ and $\mathbf{K}_g$ and the constant phase $\varphi(\mathbf{h}-\mathbf{g})$ of the structure factor $F(\mathbf{h}-\mathbf{g})$ of the coupling vector $\mathbf{h}-\mathbf{g}$. Fig. 5 shows that the phase difference $\hat{\varphi}(\mathbf{h}) - \hat{\varphi}(\mathbf{g})$ depends on ψ. This can be written as

$$\hat{\varphi}(\mathbf{h}) - \hat{\varphi}(\mathbf{g}) = \varphi(\mathbf{h}) - \varphi(\mathbf{g}) + \Delta(\psi). \quad (18)$$

$\varphi(\mathbf{h})$, $\varphi(\mathbf{g})$ are the constant phases of the structure factor $F(\mathbf{h})$, $F(\mathbf{g})$ and $\Delta(\psi)$ represents the additional phase shift. Then, by use of (1),

$$\hat{\Phi}_\Sigma = \Phi_\Sigma + \Delta(\psi). \quad (19)$$

$\Delta(\psi)$ varies from 0 to π.

The analogous phase shift occurs in the two-beam case, too. The phases of the diffracted waves, belonging to the α or β branch, differ by π, independent of the phase of the structure factor. When a r.l.p. N involved in a two-beam case is inside the Ewald sphere, essentially tiepoints on the β branch are active, *i.e.* the phase between $\mathbf{D}_0$ and $\mathbf{D}_n$ is equal to $\varphi(\mathbf{n})$. When N is outside the sphere, tiepoints on the α branch are active and the phase $\varphi(\mathbf{n})$ is shifted by π (Batterman & Cole, 1964).

The asymmetry of the rocking-curve profile can now be explained as follows. When G lies outside the Ewald

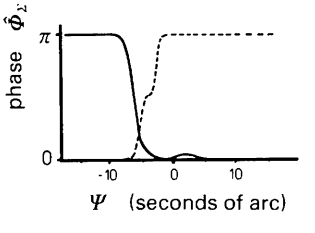

Fig. 5. Calculated phase sum $\hat{\Phi}_\Sigma$ for a positive (dashed line) and a negative triplet (full line) for one polarization only; Bragg–Bragg case of Fig. 4.

sphere ($\psi < 0$) the interference for a positive triplet ($\Phi_\Sigma = 0$) will be constructive ($\hat{\Phi}_\Sigma = 0$). Since the amplitude of the detour excited wave $[\gamma_g(\psi)D_0]$ increases when G approaches the sphere ($\psi \to 0$), the intensity first increases. Then the phase $\hat{\Phi}_\Sigma$ shifts to π and the interference becomes destructive, *i.e.* the intensity drops below the two-beam intensity. With increasing ψ the r.l.p. G leaves the sphere and the amplitude $\gamma_g(\psi)D_0$ of the detour excited wave becomes negligibly small and the observed intensity is that of the two-beam case.

For a negative triplet ($\Phi_\Sigma = \pi$) the situation is completely reversed. When G is outside the sphere ($\psi < 0$) there is no additional phase shift [$\Delta(\psi) = 0$]. Thus $\hat{\Phi}_\Sigma = \pi$, that means the direct and detour excited wave have opposite phases. But for $\psi > 0$ it is $\Delta(\psi) = \pi$ and $\hat{\Phi}_\Sigma = 0$, that means both waves have equal phases. Therefore the observed intensity is first decreased below and then increased above the two-beam intensity level. Hence, comparing the intensity profiles of the same reflection **h** involved in a three-beam case with a positive or negative triplet the following inequalities hold:

$$I_h^+(-\psi) > I_h^-(-\psi); \quad I_h^+(\psi) < I_h^-(\psi).$$

The interference phenomena discussed above give a physical interpretation of some effects contained in the fundamental equations of the dynamical theory. It should be pointed out that the superposition of the exit waves leads to the *Pendellösung* phenomenon and to the spatial distribution of the diffracted intensities within the fan of beams. These effects are not considered in this paper. Whether the intensities of the amplitudes add for the exit beams depends on the choice of the exit boundary conditions (Batterman & Cole, 1964) and therefore on the experimental conditions (*cf.* § 2*c*).

We gratefully acknowledge useful discussions with Professor H. Burzlaff.

References

ALEXANDER, L. E. & SMITH, G. S. (1962). *Acta Cryst.* **15**, 983–1004.

BATTERMAN, B. W. & COLE, H. (1964). *Rev. Mod. Phys.* **36**, 681–717.

BILLY, H. & HÜMMER, K. (1981). *Z. Kristallogr.* **156**, 114.

CHANG, S. L. (1982). *Phys. Rev. Lett.* **48**, 163–166.

CHAPMAN, L. D., YODER, D. R. & COLLELA, R. (1981). *Phys. Rev. Lett.* **46**, 1578–1581.

COLLELA, R. (1974). *Acta Cryst.* A**30**, 413–423.

EWALD, P. P. & HÉNO, Y. (1968). *Acta Cryst.* A**24**, 5–15.

HART, M. & LANG, A. R. (1961). *Phys. Rev. Lett.* **7**, 120–121.

HILDEBRANDT, G. (1967). *Phys. Status Solidi*, **24**, 245–261.

JAMES, R. W. (1948). *The Optical Principles of the Diffraction of X-Rays; The Crystaline State*, Vol. II, pp. 312–315. London: Bell.

KAMBE, K. (1957). *J. Phys. Soc. Jpn*, **12**, 13–31.

KISHINO, S. & KOHRA, K. (1971). *Jpn. J. Appl. Phys.* **10**, 551–557

LAUE, M. VON (1960). *Röntgenstrahl-Interferenzen*, 3rd ed., p. 310. Frankfurt am Main: Akademische Verlagsgesellschaft.

LIPSCOMB, W. N. (1949). *Acta Cryst.* **2**, 193–194.

PINSKER, Z. G. (1978). *Dynamical Scattering of X-rays in Crystals: Solid-State Sciences* 3, edited by M. CARDONA, P. FULDE & H.-J. QUEISSER. Berlin, Heidelberg: Springer Verlag.

POST, B. (1979). *Acta Cryst.* A**35**, 17–21.

Acta Cryst. (1982). A**38**, 848–854

Space-Group Determinations on β- and γ-Brasses

BY P. GOODMAN AND A. J. MORTON

CSIRO Division of Chemical Physics, PO Box 160, *Clayton, Victoria, Australia* 3168

(*Received* 25 *September* 1981; *accepted* 18 *June* 1982)

Abstract

Mixed γ-brass/β-brass samples have been examined by convergent-beam electron diffraction and electron microscopy. This study has led to the allocation of a centrosymmetric space group for the regular inversion antiphase domain superstructure of γ-brass, and also resulted in the identification of a hitherto unreported tetragonal structure for the body-centred cubic ordered β-brass. In the dual convergent-beam/microscopy examination of the γ-brass samples, images were taken from samples thick enough to give structured convergent-beam patterns. The resulting images are complicated by beam convergence to the extent where only the image symmetry can be interpreted directly.

0567-7394/82/060848-07$01.00